LBL-25608
Preprint

Lawrence Berkeley Laboratory
UNIVERSITY OF CALIFORNIA

Materials & Chemical Sciences Division

Submitted to Journal of the Electrochemical Society

Potential and Concentration Variations of a Reacting, Supporting Electrolyte

A.K. Hauser and J. Newman

July 1988

Prepared for the U.S. Department of Energy under Contract Number DE-AC03-76SF00098.

DISCLAIMER

LBL-25608

Potential and Concentration Variations of a Reacting, Supporting Electrolyte

Alan K. Hauser and John Newman

Materials and Chemical Sciences Division, Lawrence Berkeley Laboratory,
and Department of Chemical Engineering, University of California,
Berkeley, CA 94720

Abstract

Steady-state electrolytic mass transfer to a rotating disk has been characterized in dilute solutions with an excess of supporting electrolyte. This limiting case yields an analytic solution for the concentration variations of the electrolyte. Several electrode reactions are investigated using this approach, with emphasis on systems where the major ions of the supporting electrolyte participate in the electrochemical reaction.

When the supporting electrolyte participates in the electrode reaction, it is difficult *a priori* to predict accurately the shape of the concentration profiles. For example, the direction that a species migrates due to the gradient of the electric field may be contradictory to what is intuitively expected. The model predicts in certain cases that cations migrate to/away from the anode/cathode as opposed to being attracted to/rejected from the electrode surface. However, the analytically calculated concentration-difference ratios enable the profiles next to the disk to be sketched qualitatively, and comparisons then can be made with the numerically calculated concentration profiles. Additionally, profiles for conditions with less supporting electrolyte can be predicted from this limiting-case ratio and provide insight for

keywords: rotating disk, dilute-solution theory, potential minima

understanding the effect that migration has on the current.

Finally, in three of four systems investigated for this paper, the model predicts unexpected maxima in the counterion concentration profile. An explanation for this interesting behavior is presented in terms of the speed at which the species move, according to the magnitude of their diffusion coefficients. Alternatively, examination of the diffusion potential yields insight into this occurrence and the corresponding minima in the potential.

1. Introduction

To assess reliably and completely the contribution of migration, it is necessary to solve simultaneously the coupled, nonlinear governing differential equations for electrolytic mass transfer.[1] This of course requires a numerical solution to the problem and previously has been done.[2] The concentration variation of the supporting electrolyte also was calculated[3] as a by-product of the determination of the effect of migration on limiting currents for the rotating disk.

In the limit of an excess of supporting electrolyte, however, the effect of migration must be considered for only the major ions of the electrolyte. Thus, it is possible to obtain an analytic solution to the governing equations for the concentration variation of the electrolyte. An advantage of this limiting-case approach is that the analytic solution, expressed as concentration-difference ratios, provides quick and useful results about a given electrochemical system. Applications of this method will be demonstrated in this paper for various systems that have a reacting supporting electrolyte.

2. Model Development

The mathematical model to be discussed accounts for the one-dimensional transport processes occurring next to a rotating-disk electrode under steady-state conditions. The purpose of this paper, as in reference [4], is to present the analytic solution to the governing equations and to determine the concentration and potential profiles in the limit of a large excess of supporting electrolyte.

2.1. Minor Species

The steady-state mass balance[3] for a minor constituent i reduces to

$$3\xi^2\frac{dc_i}{d\xi} + \frac{D_i}{D_R}\frac{d^2c_i}{d\xi^2} = 0 \quad , \tag{1}$$

when migration can be neglected in the limit of a large excess of supporting electrolyte. The axial distance variable from the disk, z, has been made dimensionless using the diffusion-boundary layer thickness, δ_R; thus,

$$\xi = \frac{z}{\delta_R} \quad , \quad \text{where} \quad \delta_R = \left(\frac{3D_R}{a\nu}\right)^{1/3}\left(\frac{\nu}{\Omega}\right)^{1/2} \quad . \tag{2}$$

D_R is the diffusion coefficient of the reference (limiting reactant) species, ν is the kinematic viscosity, Ω is the angular rotation speed, and $a = 0.51023262$. A one-term axial velocity profile, $v_z = -a\Omega(\Omega/\nu)^{1/2}\, z^2$, has been used here, valid only for large values of the Schmidt number.

The minor components are found by solving the resulting equation of convective diffusion with the following boundary condition. At the electrode surface, the flux of species i is related to the normal current density i_n to the disk by Faraday's law

$$N_i = -D_i \frac{dc_i}{dz}\bigg|_{z=0} = -\frac{s_i i_n}{nF} \quad , \tag{3}$$

where the migration terms are neglected for the minor species. All of the minor ionic species are either a reactant or a product in the single electrode reaction represented by the generalized equation

$$\sum_i s_i M_i^{z_i} \rightarrow n e^- \quad . \tag{4}$$

The solution to equation 1 with boundary condition 3 yields

$$c_i(\xi) - c_{i,\infty} = \frac{s_i i_n}{nF} \frac{\delta_R}{D_i} \int_{\infty}^{\xi} e^{-x^3 D_R/D_i} dx \tag{5}$$

for the concentration profile of any minor species i, when electric-field effects are not considered.

The ratio of the concentration difference of all minor species i relative to the reference species concentration difference is an important quantity for characterizing the mass transport to the disk. The concentration profile provides the relationship

$$\frac{c_{i,0} - c_{i,\infty}}{c_{R,0} - c_{R,\infty}} = \frac{s_i}{s_R} \left(\frac{D_R}{D_i} \right)^{2/3} \quad . \tag{6}$$

This concentration-difference ratio for the minor species depends only on diffusion and stoichiometric coefficients in the absence of a strong electric field. A great economy in computation can be achieved by using equation 6 to find the concentrations of all minor species.

2.2. Supporting Electrolyte

The linearized material balances, accounting for migration, for the added and counterions are as follows

$$3\xi^2\frac{dc_1}{d\xi}+\frac{D_1}{D_R}\left[\frac{d^2c_1}{d\xi^2}+z_1\frac{d}{d\xi}\left(c_1^0\frac{d\phi}{d\xi}\right)\right]=0 \quad , \tag{7}$$

$$3\xi^2\frac{dc_2}{d\xi}+\frac{D_2}{D_R}\left[\frac{d^2c_2}{d\xi^2}+z_2\frac{d}{d\xi}\left(c_2^0\frac{d\phi}{d\xi}\right)\right]=0 \quad , \tag{8}$$

where c_1^0 and c_2^0 are the uniform concentrations of these ions supposed to prevail in the absence of any reaction. The concentrations satisfy the electroneutrality relations in the form

$$z_1c_1+z_2c_2+\sum_{i=3}z_ic_i=0 \quad , \tag{9}$$

$$z_1c_1^0+z_2c_2^0=0 \quad , \tag{10}$$

where the sum is for all minor species that participate in the electrode reaction. Elimination of the dimensionless potential $\phi=F\Phi/RT$ and the counterion concentration c_2 from equations 7 and 8 using equations 9 and 10, therefore, yields for the added ion

$$\left(1-\frac{z_1}{z_2}\right)\left(\frac{d^2c_1}{d\xi^2}+3\xi^2\frac{D_R}{D_e}\frac{dc_1}{d\xi}\right)=\sum_{i=3}\frac{z_i}{z_2}\left(1-\frac{D_i}{D_2}\right)\left(\frac{d^2c_i}{d\xi^2}\right) \quad , \tag{11}$$

where

$$D_e=\frac{D_1D_2(z_1-z_2)}{z_1D_1-z_2D_2} \quad . \tag{12}$$

Substitution of equation 5 for the concentration profile of the minor species i into equation 11 results in the following governing equation for the concentration of the added ion 1

$$\left(1-\frac{z_1}{z_2}\right)\left(\frac{d^2c_1}{d\xi^2}+3\xi^2\frac{D_R}{D_e}\frac{dc_1}{d\xi}\right)$$
$$=\sum_{i=3}\frac{z_i}{z_2}\left(1-\frac{D_i}{D_2}\right)\left[\frac{s_i i_n}{nF}\frac{\delta_R}{D_i}\left(-3\xi^2\frac{D_R}{D_i}\right)e^{-\xi^3 D_R/D_i}\right] \quad . \tag{13}$$

The solution of equation 13 for species 1 satisfying the boundary condition at infinity, $c_i = c_{i,\infty}$, is

$$c_1(\xi) = c_{1,\infty} + \sum_{i=3,4}\frac{z_i}{z_2-z_1}\frac{\frac{D_i}{D_2}-1}{\frac{D_i}{D_e}-1}\left[\frac{s_i i_n}{nF}\frac{\delta_R}{D_i}\int_\infty^\xi e^{-x^3 D_R/D_i}dx\right]$$
$$+ B\int_\infty^\xi e^{-x^3 D_R/D_i}dx \quad . \tag{14}$$

The boundary condition at the electrode is that the flux of ions 1 and 2 is not zero, as for the usual case, but instead is proportional to the current density given by

$$\frac{dc_1}{d\xi}+z_1c_1^0\frac{d\phi}{d\xi}=\frac{s_1 i_n}{nF}\frac{\delta_R}{D_1} \quad , \tag{15}$$

and

$$\frac{dc_2}{d\xi}+z_2c_2^0\frac{d\phi}{d\xi}=\frac{s_2 i_n}{nF}\frac{\delta_R}{D_2} \quad . \tag{16}$$

This is a modification of equation 3 with inclusion of the migration term for the major ionic species. Elimination of the potential derivative and the use of the electroneutrality equations 9 and 10 allow the boundary condition to be written as

$$\frac{dc_1}{d\xi}\left(1-\frac{z_1}{z_2}\right)=\sum_{i=3,4..}\frac{z_i}{z_2}\frac{dc_i}{d\xi}+\frac{i_n}{nF}\left(\frac{s_1}{D_1}+\frac{s_2}{D_2}\right)\delta_R$$

$$=\sum_{i=3,4..}\frac{z_i}{z_2}\frac{s_i i_n}{nF}\frac{\delta_R}{D_i}+\frac{i_n}{nF}\left(\frac{s_1}{D_1}+\frac{s_2}{D_2}\right)\delta_R \tag{17}$$

at $\xi = 0$. This allows the determination of the constant B in equation 14:

$$B=\frac{\frac{i_n}{nF}\delta_R}{\left(z_2-z_1\right)}\left\{z_2\left(\frac{s_1}{D_1}+\frac{s_2}{D_2}\right)-\sum_{i=3,4}\frac{z_i s_i}{D_i}\left[\frac{\frac{D_i}{D_2}-1}{\frac{D_i}{D_e}-1}\right]\right\} \tag{18}$$

We can calculate the concentration change of the added ion 1 between the bulk and the electrode surface relative to that of the reference species by substituting the integration constant B into the concentration profile of species 1. Finally, use of equations 14 and 18 and rearrangement yields

$$\frac{c_{1,0}-c_{1,\infty}}{c_{R,0}-c_{R,\infty}}=\left(\frac{D_e}{D_R}\right)^{1/3}\frac{z_2}{z_2-z_1}\frac{D_R}{s_R}\left(\frac{s_1}{D_1}+\frac{s_2}{D_2}\right)$$

$$+\sum_{i=3,4}\frac{z_i}{z_2-z_1}\frac{s_i}{s_R}\left\{\frac{\frac{D_i}{D_2}-1}{\frac{D_i}{D_e}-1}\left[1-\left(\frac{D_e}{D_i}\right)^{1/3}\right]+\left(\frac{D_e}{D_i}\right)^{1/3}\right\}\left(\frac{D_R}{D_i}\right)^{2/3} \tag{19}$$

The corresponding equation for c_2 can be obtained from equation 19 by reversing the subscripts 1 and 2. The second term on the right of equation 19 is the same as equation 121-19 of reference [3]. The first term accounts for the electrolyte species participating in the electrochemical reaction.

3. Results

Four electrochemical reactions are presented in this section, where the supporting electrolyte is either consumed or produced at the rotating disk. Concentration and potential profiles are to be given, and differences that arise due to different numbers of electrons being transferred in the reactions will be examined. The concentration as a function of the dimensionless distance ξ from the rotating-disk electrode could be obtained by integrating equations 5 and 14 for the minor species and the supporting-electrolyte ions, respectively. The MIGR program[3] is used instead for a large excess of supporting electrolyte ($r = -z_1 c_{1,\infty}/z_2 \cdot c_{2,\infty} = 0.99$).

3.1. $KAuCl_4$ - KCl System

The deposition-of-gold reaction in a $KAuCl_4$-KCl electrolyte is given by

$$AuCl_4^- + 3e^- \rightarrow Au + 4Cl^- \quad , \tag{20}$$

where the gold chloride complex $AuCl_4^-$ is consumed at the electrode, and the added chloride ion is produced at the surface. The concentration variations of the electrolyte for this reaction are presented in table 1. The concentration-difference ratios, $\frac{c_{i,0} - c_{i,\infty}}{c_{R,0} - c_{R,\infty}}$, that are tabulated are given by equation 19 and are independent of the bulk concentration of all the species. The ratios are a function of only the charge numbers, stoichiometric coefficients, and diffusion coefficients of the species, and the values of these parameters may be found in the table along with the analytic limit of each species i written relative to the $AuCl_4^-$ reference ion ($R = 3$).

Table 1. Analytic results of the concentration variation of the supporting electrolyte for the deposition of gold and cogeneration of Cl^- in an excess of KCl supporting electrolyte.

no.	species i	z_i	s_i	$D_i \times 10^5$ (cm^2/s)	$\frac{c_{i,0} - c_{i,\infty}}{c_{R,0} - c_{R,\infty}}$
1	Cl^-	-1	4	2.032	-1.3234
2	K^+	1	0	1.957	-0.3234
R=3	$AuCl_4^-$	-1	-1	0.540	1.0

The concentration profiles of each of the species as a function of ξ from the disk are given in figure 1, where the chloride diffusion coefficient is used to scale the problem enabling the diffusion layers of all the species to be within the distance domain, $\xi_{max} = 2.0(D_{max}/D_R)^{1/3}$. Although the analytic results for the concentration variations of the electrolyte are valid for any fraction below the limiting current, the profiles in the figure and the following discussion pertain to the limiting-current case only. We should first examine the concentration difference of the reference gold chloride complexed species. At the cathodic limiting current, the concentration of the limiting reactant is zero at the disk surface, resulting in a negative concentration difference, $c_{R,0} - c_{R,\infty}$. Additionally, the magnitude of the difference is small since in order for equation 19 to be valid for the major species, the bulk concentration of the minor species must be much less than that of the supporting electrolyte.

Next, let us look at the concentration-difference ratios of the supporting electrolyte shown in the same figure. The ratios of the Cl^- added ion and the K^+ counterion are

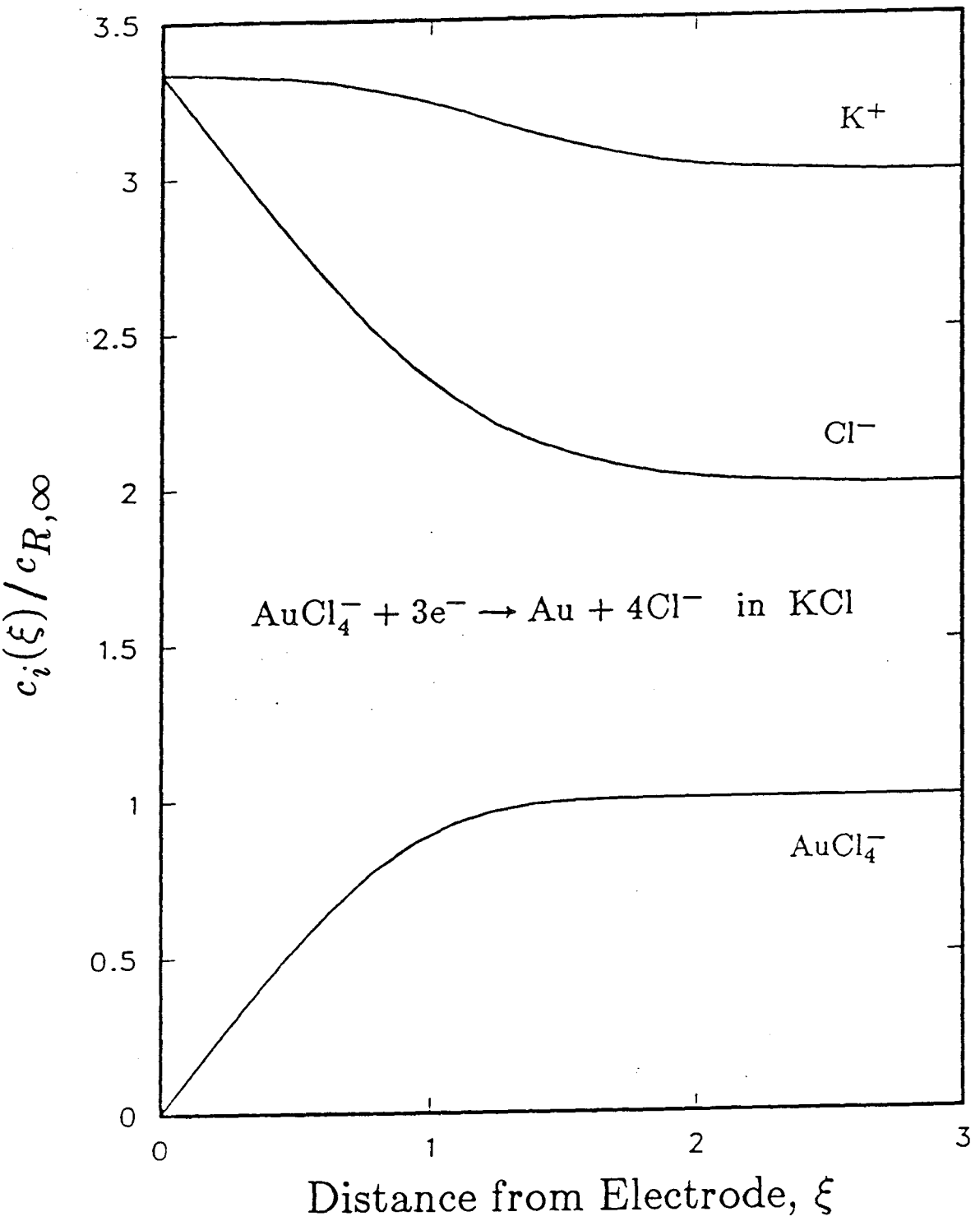

Figure 1. Concentration profiles for the cathodic reduction of $AuCl_4^-$ at the limiting current in an excess of KCl supporting electrolyte. A constant has been added to the concentration ratios for the K^+ and Cl^- ions so that they can be plotted together with the limiting reactant but otherwise undistorted.

-1.323 and -0.323, respectively. Chloride ions are generated at the cathode, thus overriding any repulsive migrational effect and producing a negative concentration-difference ratio. The absolute value of the ratio is greater than one because the chloride concentration difference is larger than the change in the limiting-reactant concentration due to the stoichiometric amount of chloride that is generated (four times the amount of $AuCl_4^-$ consumed).

The concentration difference across the diffusion layer of the counterion is determined by interchanging the subscripts 1 and 2 in equation 19. The overall result, as seen in figure 1, is summarized by

$$c_{2,0} = c_{1,0} > c_{2,\infty} = (c_A + c_B) \quad , \tag{21}$$

where c_A and c_B are the bulk concentrations of the KCl supporting electrolyte and the $KCuCl_2$ electrolyte, respectively. The bulk concentration of K^+, $c_{2,\infty}$, is determined by specifying c_A and c_B. The surface concentration of the nonreacting K^+, $c_{2,0}$ is dictated by the surface concentration of the chloride ion being generated in the electrochemical reaction, $c_{1,0}$. At limiting current, the surface concentrations of the added and counterions are the same due to electroneutrality. Hence, the concentration difference of potassium is positive, giving a negative concentration-difference ratio. This result agrees with what is expected since the potassium ion should be electrically attracted to the cathode yielding a higher surface concentration than in the bulk. Finally, the magnitude of this effect reflects the concentration change of the reacting added ion as a result of electroneutrality; thus, the ratio is significantly less than one.

3.2. $KCuCl_2$ - KCl System

The deposition of copper and simultaneous generation of chloride ions from cuprous chloride in a supporting potassium chloride electrolyte occurs by the overall reaction

$$CuCl_2^- + e^- \rightarrow Cu + 2Cl^- \quad . \tag{22}$$

Analytic results of the concentration variation of the supporting electrolyte are summarized in table 2 for this system in an excess of KCl supporting electrolyte. Transport properties identical to the gold system have been used. The only difference between the two cases is the stoichiometry and thus the number of electrons involved in the electrochemical reactions.

The concentration profiles are shown in figure 2 at the limiting current. The concentration difference, $c_{R,0} - c_{R,\infty}$ is negative for the limiting reactant, as for the previous case. The added Cl^- ion is produced in the reduction reaction and therefore

Table 2. Analytic results of the concentration variation of the supporting electrolyte for the deposition of copper and cogeneration of Cl^- in an excess of KCl supporting electrolyte.

no.	species i	z_i	s_i	$D_i \times 10^5$ (cm^2/s)	$\frac{c_{i,0} - c_{i,\infty}}{c_{R,0} - c_{R,\infty}}$
1	Cl^-	-1	2	2.032	-0.9126
2	K^+	1	0	1.957	0.0874
R=3	$CuCl_2^-$	-1	-1	0.540	1

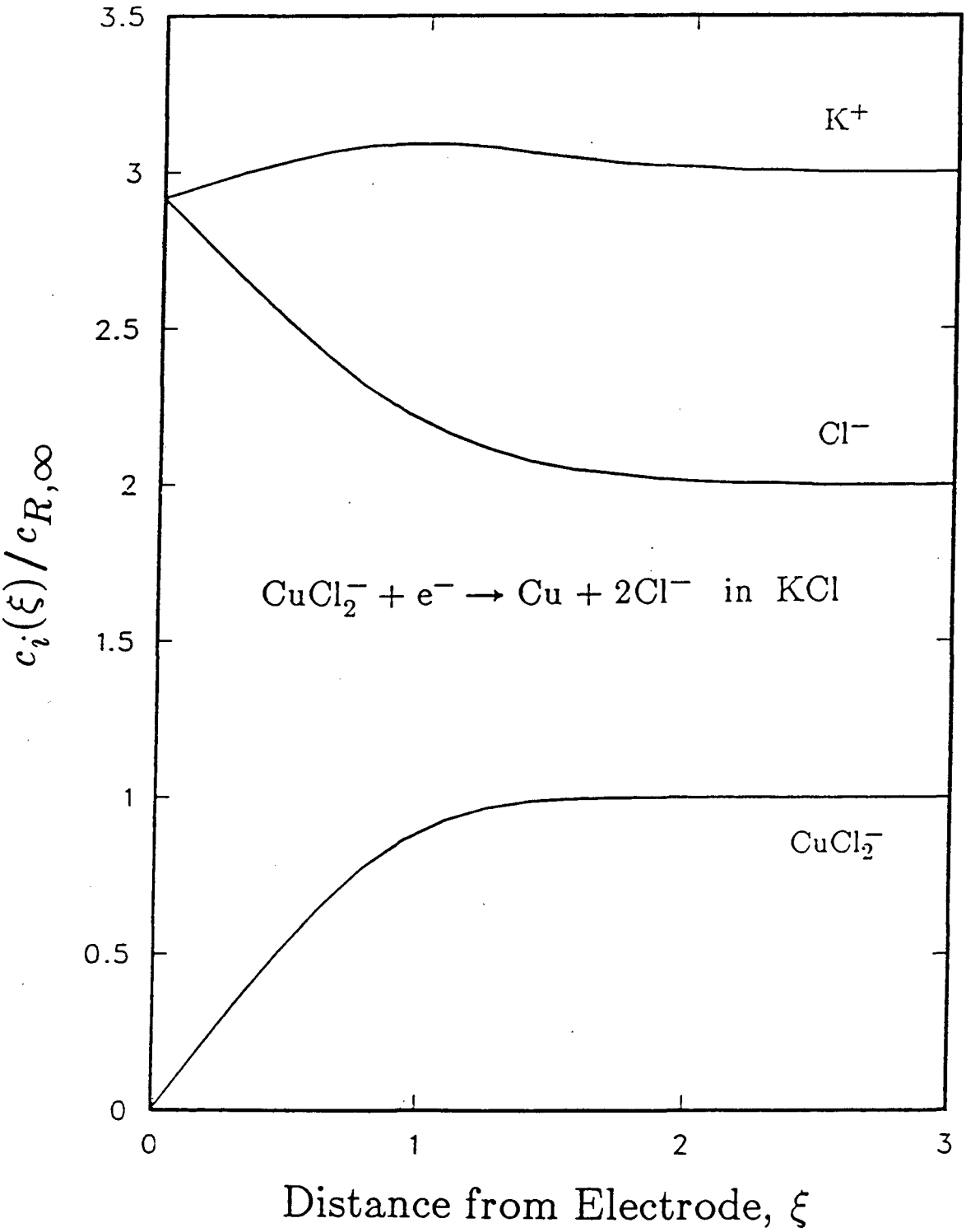

Figure 2. Concentration profiles for the cathodic reduction of $CuCl_2^-$ at the limiting current in an excess of KCl supporting electrolyte. A constant has been added to the concentration ratios for the K^+ and Cl^- ions so that they can be plotted together with the limiting reactant but otherwise undistorted.

has a positive concentration difference and a negative concentration-difference ratio. The absolute value of the ratio is just less than one. This is somewhat unexpected, since two chlorides are generated for each cuprous chloride being consumed. This should yield a larger concentration difference than that of the limiting reactant, and thus a ratio greater than one, as for the gold deposition reaction. Let us discuss this further.

The stoichiometry of the reaction and the magnitude of the diffusion coefficients are such that the concentration-difference ratio of the K^+ counterion is positive because

$$c_{2,\infty} = (c_A + c_B) > c_{2,0} = c_{1,0} \quad . \tag{23}$$

This again contradicts what intuition would tell us about the concentration difference as determined by migration. For example, in a nonreacting system, positive ions are expected to migrate toward the cathode yielding a positive concentration difference. This conflict with intuition manifests itself in equation 19 for reacting supporting-electrolyte systems where s_i and D_i dictate the overall behavior.

Another interesting and unexpected feature of the copper chloride system that is illustrated in figure 2 is the maximum in the K^+ concentration profile that occurs at a dimensionless distance of $\xi = 1$ or 1.2×10^{-3} cm (12 microns). Although we are interested in analyzing this profile in an attempt to explain the maximum, we must keep in mind that solute species do not diffuse independently in electrolytic solutions. Instead, a significant diffusion potential is set up, even in the absence of current, as given by the second term in the following equation

$$\Phi = -\int_b^z \frac{i_n}{\kappa}\, dz - F \int_b^z \sum_j \frac{z_j D_j}{\kappa} \frac{\partial c_j}{\partial z}\, dz \quad , \tag{24}$$

where the first term on the right is the Ohm's law contribution to the total potential

and

$$\kappa = \frac{F^2}{R\,T} \sum_i z_i^2 D_i c_i \quad . \tag{25}$$

The diffusion potential results from the ability of certain species to diffuse more easily than others, enabling them to diffuse ahead. For example, in this case, the potassium and chloride ions move faster than the $CuCl_2^-$ ions, since their diffusion coefficients are almost four times larger, and this yields a KCl diffusion layer which is thicker than that of $KCuCl_2$.† Consequently, the ions interact with the established diffusion potential as seen in figure 3, where the concentration maximum in figure 2 corresponds to the minimum in potential in figure 3. Although the profiles of the concentration-difference ratios are independent of the magnitude of the concentration and rotation speed, the potential profiles, relative to the zero of potential at ξ_{max}, do depend on these variables. Thus, for the gold and copper deposition cases, $r = c_A/(c_A + c_B) = 0.99$, where $c_A = 0.02$ mol/cm^3 KCl and $c_B = 2.02\times10^{-4}$ mol/cm^3 $KMCl_x$. The disk rotation speed is 1600 rpm for all systems investigated in this paper. Let us now examine the potential profiles more closely.

According to equation 24, if all the diffusion coefficients are the same, then the diffusion potential term is zero. When $\Delta\Phi_{diff}$ is small, we should expect the gradient of potential and the current to be of opposite sign, as for the gold deposition case. That is, for a cathode we should expect the potential gradient to be positive and positively

† The ability of ions to move at different rates yielding significantly different electrolyte diffusion-layer thicknesses was experimentally detected for the copper sulfate and sulfuric acid system. An optical interference method was used to measure the refractive index, and a maximum was displayed by this system in a stagnant diffusion cell since the diffusion layer for H_2SO_4 is thicker than that for $CuSO_4$.[5]

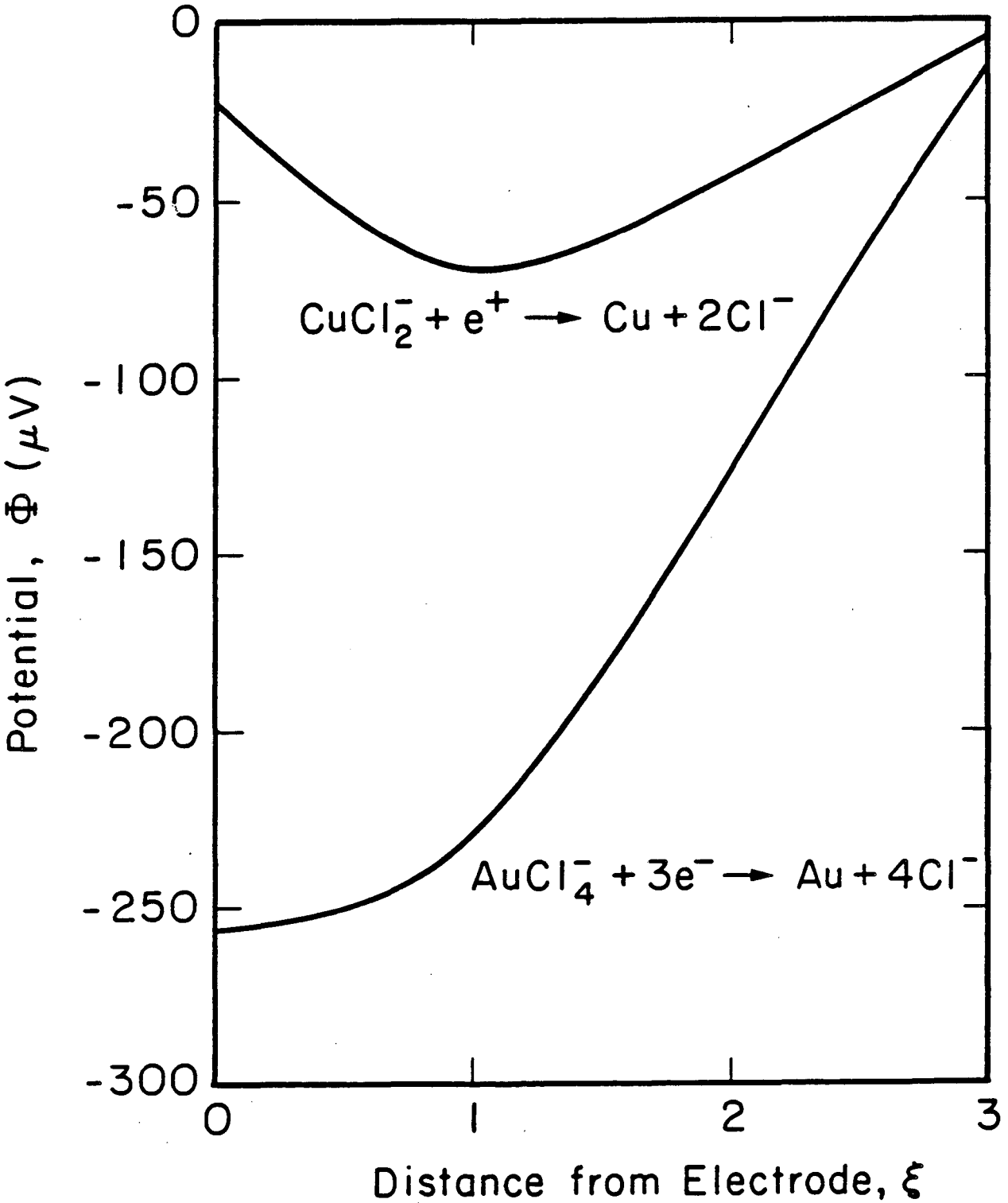

Figure 3. Potential profiles for gold and copper deposition at the limiting current in an excess of potassium chloride ($r = 0.99$), $c_A = 0.02$ mol/cm^3 KCl, $c_B = 2.02 \times 10^{-4}$ mol/cm^3 $KMCl_z$, and $\Omega = 1600$ rpm.

charged ions to migrate to the electrode surface. However, contrary to this expected behavior, the potential gradient is negative near the copper cathode, and the K^+ concentration increases from the surface, before going through a maximum.

This unexpected behavior confirms the importance of the diffusion potential term in equation 24 for the potential variation within the solution. $\Delta\Phi_{diff}$ dominates next to the electrode, whereas the ohmic term dictates further away from the electrode. Consequently, farther into the solution, the concentration of potassium decreases as migration predicts. Finally, the potential profiles shown in the figure clearly indicate that the current is three times higher for the gold system, making it more difficult for the diffusion potential to reverse the sign of $\nabla\Phi$.

3.3. $K_2Zn(OH)_4$ - KOH System

The deposition of zinc in alkaline solutions is written here as the reduction of $Zn(OH)_4^{2-}$

$$Zn(OH)_4^{2-} + 2e^- \rightarrow Zn + 4\ OH^- \qquad (26)$$

because the zincate ion is the only zinc hydroxide complex of importance in KOH battery electrolytes.[6] Hydroxide ions, the added ion of the supporting electrolyte, are also generated in this reaction. Analytic results from equation 19 for the concentration variation of the zincate reduction reaction are summarized in table 3. Although zinc concentration profiles are not included here, the calculated ratios in the table can be used to map out the concentration profiles. The concentration difference of the added hydroxide ion changes more than that of the reference ion across the boundary layer because four times as much OH^- is being generated as $Zn(OH)_4^{2-}$ is consumed. Thus,

Table 3. Analytic results for the concentration variation for the cathodic discharge of zincate in $K_2Zn(OH)_4$ and an excess of KOH supporting electrolyte.

no.	species i	z_i	s_i	$D_i \times 10^5$ (cm^2/s)	$\frac{c_{i,0} - c_{i,\infty}}{c_{R,0} - c_{R,\infty}}$
1	OH^-	-1	4	5.26	-1.1503
2	K^+	1	0	1.957	0.8496
3=R	$Zn(OH)_4^{2-}$	-2	-1	0.10	1.0

the hydroxide ratio is negative, and its absolute value is greater than one. In this case, although the surface concentration of hydroxide is large, the concentration-difference ratio of potassium is positive because

$$c_{2,\infty} = (c_A + 2c_B) > c_{2,0} = c_{1,0} \quad . \tag{27}$$

At the limiting current, the concentration of potassium and hydroxide increase and decrease, respectively, from the same concentration at the surface to their specified bulk values. These profiles are similar to the supporting electrolyte profiles in the copper system; a concentration maximum occurs for the potassium counterion. The potential profile is given in figure 4 for $r = c_A/(c_A + 2c_B) = 0.99$, where $c_A = 19.8$ mol/cm^3 KOH, $c_B = 0.1$ mol/cm^3 $K_2Zn(OH)_4$. Again, a minimum is seen.

3.4. Nitrate Reduction in Acidic Nickel Nitrate

Next, we give results of the present analysis characterizing the cathodic behavior of a rotating disk in nickel nitrate solutions. Nickel hydroxide, the active material in

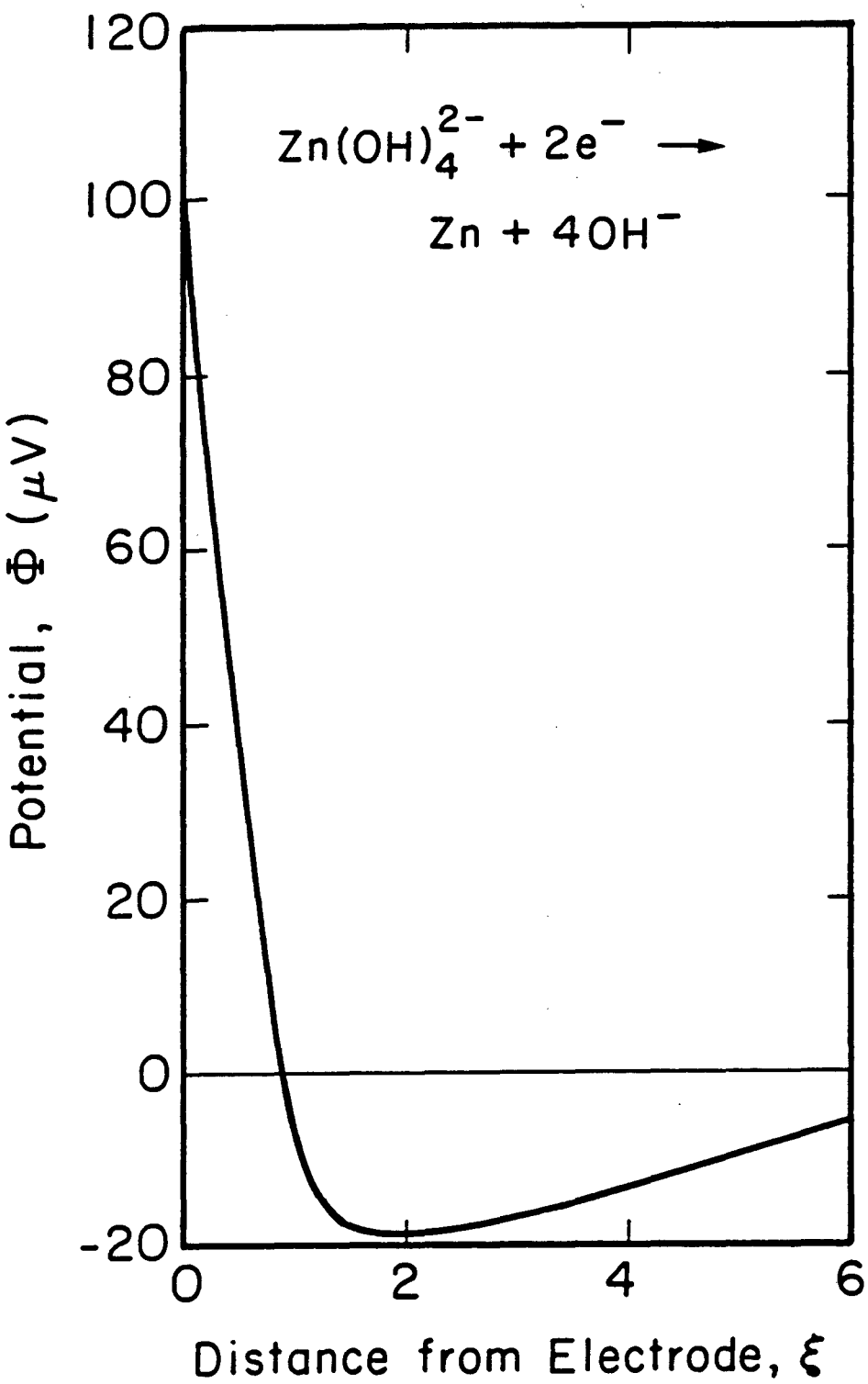

Figure 4. Potential profile as a function of the dimensionless distance ξ from the rotating disk ($\Omega = 1600$ rpm) for zincate reduction at the limiting current in an excess of KOH supporting electrolyte ($c_A = 19.8$ mol/cm^3 KOH and $c_B = 0.1$ mol/cm^3 $K_2Zn(OH)_4$).

nickel battery electrodes, is precipitated by the following reaction

$$Ni^{++} + 2H_2O \rightarrow NiOH_2 + 2H^+ \quad . \tag{28}$$

In this investigation, however, we study the nickel nitrate system at conditions in which $NiOH_2$ precipitation is not initiated. That is the solution adjacent to the electrode is not sufficiently alkaline for precipitation of nickel hydroxide or any of the other basic nickel salts. Thus, the electrochemical process just prior to the formation of a $NiOH_2$ film on the disk electrode is of interest. The nitrate reduction reaction is given by

$$NO_3^- + 3H^+ + 2e^- \rightarrow HNO_2 + H_2O \quad , \tag{29}$$

where HNO_2 is the principal reaction product in concentrated nickel nitrate solutions.[7]

The concentration-difference ratios are presented in table 4 for H^+, NO_3^-, and Ni^{2+} species prior to the onset of chemical precipitation of nickel hydroxide. The minor reacting hydrogen cations are consumed at the limiting current at the cathode, while the nitrate counterions are simultaneously reduced. This system is slightly different from the previous ones because the reacting ion of the supporting electrolyte, NO_3^-, is the

Table 4. Analytic concentration-variation results for the reduction of nitrate in an excess of $Ni(NO_3)_2$ supporting electrolyte.

no.	species i	z_i	s_i	$D_i \times 10^5$ (cm^2/s)	$\frac{c_{1,0} - c_{1,\infty}}{c_{R,0} - c_{R,\infty}}$
1	Ni^{2+}	2	0	0.75	0.00951
2	NO_3^-	-1	-1	1.902	1.019
R=3	H^+	1	-3	9.312	1.0

counterion as opposed to being the added ion. Thus, a more detailed description will be given than for the zinc system.

In this case, both profiles increase as a function of distance from the electrode. Because an excess of $Ni(NO_3)_2$ supporting electrolyte is present ($r = 2c_A/(2c_A + c_B) = 0.999$), the concentration difference of the NO_3^- counterion is small relative to its bulk concentration. Additionally, the surface concentration of the Ni^{2+} added ion is of the same order of magnitude as its bulk concentration, $c_{Ni^{2+},\infty}$. Finally, the nickel cation goes through a concentration maximum, as indicated by the potential minimum in figure 5, although this overall effect is small.

The analysis of the maximum in the Ni^{2+} concentration profile also contradicts what is intuitively expected; the migration flux (at $z = 0$) contributes to the transport of Ni^{2+} away from the cathode. Again, this conflict with intuition can be resolved by examining the potential profile given by equation 24.

At the electrode surface, the magnitude and direction of the potential gradient are dominated by the diffusion potential term. The H^+ and NO_3^- are the major contributors to this potential, due to their large diffusion coefficients relative to Ni^{2+}. The ohmic term and the diffusion potential term cancel at approximately 20 microns ($\xi = 0.6$) from the electrode, resulting in the observed minimum in the electric potential. Farther into the solution, the potential gradient is determined by the Ohm's law term in the equation. At the edge of the diffusion layer, where the concentration gradients approach zero, the gradient of the diffusion potential approaches zero. Thus, the maximum in the concentration profile of the nickel species is explained by the behavior of the potential profile, since its concentration profile corresponds to the potential

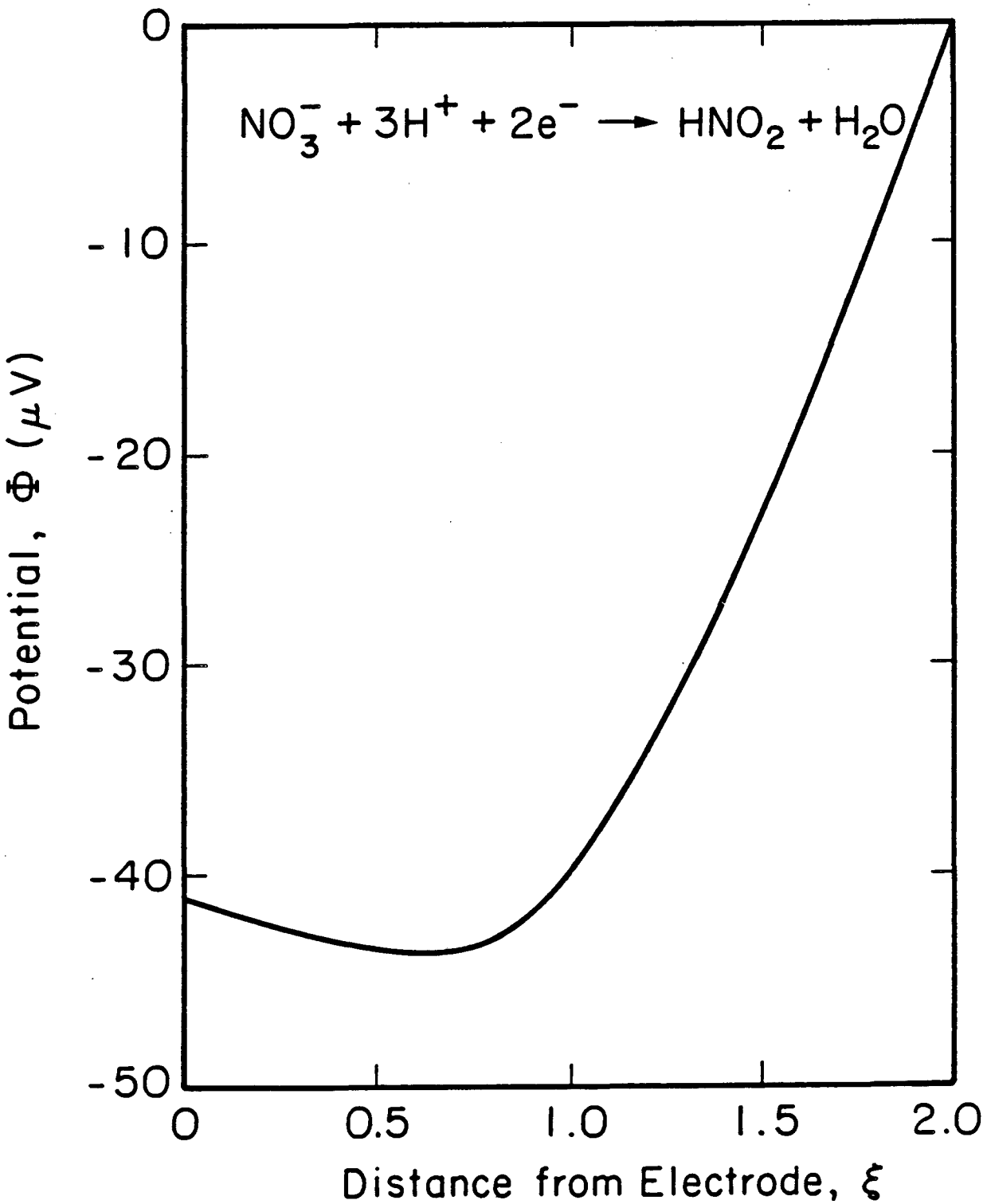

Figure 5. Potential profiles for nitrate reduction at the limiting current in an excess of $Ni(NO_3)_2$ ($r = 0.999$), $c_A = 2.56$ mol/cm^3 $Ni(NO_3)_2$, $c_B = 0.005$ mol/cm^3 HNO_3, and $\Omega = 1600$ rpm.

profile.

4. Discussion of Results

In general, if the supporting electrolyte is not involved in the electrode reaction, migration alone determines the added and counterion profiles. For example, anions/cations are attracted to the anode/cathode dictating the concentration profiles. This typical behavior is illustrated by the ferricyanide/ferrocyanide redox couple in KCl,[8] although the K^+ counterion displays a concentration maximum corresponding to a potential minimum for the cathodic reduction process. Again, the potential minimum arises due to differences in the ionic diffusion coefficients, which yield a significant diffusion potential. Examination of the concentration-difference ratios reported in reference 3 for nonreacting supporting-electrolyte systems verifies that the concentration difference for the added ion of valence one is roughly half that of the reactant ion when an excess of supporting electrolyte is present. This rule of thumb is not true for systems where the supporting electrolyte is engaged in the electrode reaction, as has been demonstrated here.

When the supporting electrolyte participates in the electrochemical reaction, it is difficult to know correctly *a priori* the shape of the concentration profiles. Ionic migration alone does not determine the shape of the profiles; instead, the stoichiometry of the reaction, magnitude of diffusion coefficients, and electroneutrality dictate the concentration of the ions as a function of distance from the electrode. Thus, significantly different and more interesting profiles result for these systems.

The analytically calculated concentration-difference ratios are most important because they enable the profiles next to the disk to be sketched qualitatively. The sign of the counterion ratio indicates whether the concentration at the surface is greater or less than the bulk concentration. For example, a positive ratio means that that ion's profile qualitatively looks like that of the limiting reactant (excluding any possible potential maximum). The concentration is smallest at the surface and increases away from the electrode. A negative ratio implies that the concentration is greatest at the surface and decreases away from the electrode. The magnitude of the ratio also is important. If the absolute value of the ratio is greater than one, then the concentration difference of species i is greater than the concentration variation of the reference ion, and *vice versa.*

Another interpretation of the concentration-difference ratio is possible by treating the reacting added ion as

$$c_1 = c_1^* + c_1' \quad , \tag{30}$$

the sum of a pseudo reacting added ion c_1^* and a nonreacting added ion c_1'. Equation 19 can be rewritten as The first term on the right corresponds to the reacting minor species term identical to equation 6. The second term is similar to the second term of equation

$$\frac{c_{1,0} - c_{1,\infty}}{c_{R,0} - c_{R,\infty}} = \frac{s_1}{s_R}\left(\frac{D_R}{D_1}\right)^{2/3} \tag{31}$$

$$+ \sum_i \frac{z_i}{z_2 - z_1}\frac{s_i}{s_R}\left\{\frac{\frac{D_i}{D_2} - 1}{\frac{D_i}{D_e} - 1}\left[1 - \left(\frac{D_e}{D_i}\right)^{1/3}\right] + \left(\frac{D_e}{D_i}\right)^{1/3}\right\}\left(\frac{D_R}{D_i}\right)^{2/3}$$

19, except that the sum in equation 31 includes all species, whereas the sum in equation 19 is only for minor species.

A convenient means of predicting the detailed shape of the concentration profiles is to determine whether a potential maximum/minimum† occurs for a particular system. Because of electroneutrality, we can write $\sum_i z_i \partial c_i/\partial z = 0$. With substitution of equations for the concentration gradient of species i similar to equations 15 and 16 and with rearrangement, the normal current density to the disk is related to the potential gradient by

$$i_n = \frac{nF^2}{RT} \frac{\sum_i z_i^2 c_i}{\sum_i \frac{z_i s_i}{D_i}} \left(\frac{\partial \Phi}{\partial z} \right)_{z=0} \tag{32}$$

This is a general result, valid at any fraction of the limiting current and with any bulk ratio of supporting electrolyte to reactant. Since the sum in the numerator can be estimated easily and is always positive, the sum in the denominator is critical. This latter sum is independent of composition and is known in advance. Thus, the stoichiometric coefficients, charge numbers, and magnitude of diffusion coefficients of the species participating in a particular reaction determine whether a potential maximum/minimum occurs or not. For example, the sum in the denominator in equation 32 is positive (8.7×10^4 s·cm^{-2}) for the copper deposition reaction 22, which implies that the potential gradient is reversed in comparison to Ohm's law. Equation 32

---

† Only potential minima have been presented since we have limited our discussion in this paper to cathodic reactions. However, a potential maximum occurs[9] for the anodic dissolution of copper in chloride solutions.

indicates reversal at the surface is not possible for the gold deposition reaction 20, since the summation in the denominator is negative (-1.2×10^4 s·cm^{-2}). Potential minima occurred in the zincate and the nitrate reduction cases, reflected by 2×10^6 s·cm^{-2} and 2×10^4 s·cm^{-2}, respectively; this confirms why the potential gradient for the zinc system is the greatest. Equation 32 also suggests that there will be no potential minimum or maximum if there is a single ionic species reacting.

Another application of equation 32 is to check the sensitivity of the occurrence of a potential maxima/minima with respect to the magnitude of the diffusion coefficients. Examination of the sum in the denominator of equation 32 for the copper deposition system implies that a diffusion coefficient, D_R, twice the value used in the present analysis would yield a potential profile without a minimum.

Finally, profiles for other conditions also can be predicted from the limiting-case concentration-difference ratio. Thus, insight is provided for understanding the effect that migration has on the current for systems with less supporting electrolyte and for polarization conditions below the limiting current. For example, the direction of the migrational force relative to the diffusional force dictates whether the limiting current is enhanced or suppressed.

5. Conclusions

Four different electrochemical systems with reacting supporting electrolytes have been theoretically investigated: the deposition of gold and copper from chloride solutions, zincate reduction, and the electrochemical process prior to the precipitation of a $NiOH_2$ film on a rotating disk. We have shown that two effects determine the

concentration profiles of these and other systems where the supporting electrolyte participates in the electrochemical reaction. First, the ratio of the stoichiometric and diffusion coefficients, as given by the analytic solution to the problem dictates the sign of the overall concentration difference of each species. Secondly, the effect that the diffusion potential has on the overall potential profile and its interaction with the concentration profiles determines the detailed shape of the profiles. For example, concentration maxima and corresponding potential minima were displayed by three of the four case studies presented here. The analysis of this behavior revealed that the direction that a species migrates due to the gradient of the electric field may be contradictory to what is intuitively expected. For example, the mathematical model predicted that positively charged species at the electrode surface migrate away from the cathodically polarized electrode, due to the diffusion potential.

Acknowledgements

This work was supported by the Assistant Secretary of Conservation and Renewable Energy, Office of Energy Systems Research, Energy Storage Division of the U.S. Department of Energy under Contract DE-AC03-76SF00098.

List of Symbols

a	constant = 0.51023262
c_i	concentration of species i, mol/cm^3
$c_{i,0}$	concentration of species i next to the electrode, mol/cm^3
$c_{i,\infty}$	concentration of species i in the bulk solution, mol/cm^3
c_A	bulk concentration of the supporting electrolyte, mol/cm^3
c_B	bulk concentration of the electrolyte, mol/cm^3
D_i	diffusion coefficient of species i, cm^2/s
D_i	diffusion coefficient of species i, cm^2/s
D_R	diffusion coefficient of the reference species, cm^2/s
$D_{\max}$	largest diffusion coefficient of the species, cm^2/s
D_e	effective diffusion coefficient of the supporting electrolyte, cm^2/s
e^-	symbol for the electron
F	Faraday's constant, 96,487 C/equiv
i_n	normal current density, A/cm^2
M_i	symbol for the chemical formula of species i
n	number of electrons involved in electrode reaction
N_i	flux of species i, mol/cm^{2}s
r	ratio of supporting electrolyte to total electrolyte

R	universal gas constant, 8.3143 J/mol-K
s_i	stoichiometric coefficient of species i in electrode reaction
T	absolute temperature, K
v_z	axial mass-average velocity, cm/s
z	axial position coordinate, cm
z_i	charge number of species i

Greek symbols:

δ_R	diffusion boundary layer thickness for reference species R, cm
κ	solution conductivity, ohm^{-1}-cm^{-1}
ν	kinematic viscosity, cm^2/s
ξ	dimensionless axial distance for rotating disk
ξ_{max}	maximum dimensionless axial distance for rotating disk
ϕ	dimensionless electric potential
Φ	electric potential, V
$\Delta\Phi_{diff}$	diffusion potential, V
Ω	rotation speed, rad/s

subscripts:

1	added ion
2	counterion
3	reactant ion
R	reference species
+	cation property
−	anion property

0	just outside the diffuse part of the double layer
∞	in the bulk electrolyte, where there are no concentration variations

References

[1]. John Newman, "The Effect of Migration in Laminar Diffusion Layers," *International Journal of Heat and Mass Transfer, 10,* 983-997 (1967).

[2]. John Newman, "Effect of Ionic Migration on Limiting Currents," *I&EC Fundamentals, 5,* 525-529 (1966).

[3]. John Newman, *Electrochemical Systems,* Englewood Cliffs, N. J.: Prentice-Hall, Inc., 1973.

[4]. Alan K. Hauser and John Newman, "Electrolytic Mass Transfer to a Rotating Disk in Dilute Solutions: Concentration Variations of the Reacting, Excessive Supporting Electrolyte," Abstract 545, Spring ECS Meeting, Atlanta, 1988.

[5]. Limin Hsueh, "Diffusion and Migration in Electrochemical Systems," Ph.D. thesis, UCRL-18597 (1968).

[6]. James McBreen and Elton J. Cairns, "The Zinc Electrode," *Advances in Electrochemistry and Electrochemical Engineering, 11,* 1-35, Heinz Gerischer and Charles W. Tobias, eds. (1978).

[7]. V. V. Zhdanov, K. I. Tikhonov, and A. L. Rotinyan, *Zhurnal Prikladnoi Khimii, 53,* 581-583 (1980) (English translation: "Cathodic Process on a Nickel Electrode in Nickel Nitrate Solutions," *Journal of Applied Chemistry of the U.S.S.R., 53,* 465-467 (1980).

[8]. Alan K. Hauser, unpublished results.

[9]. Alan K. Hauser and John Newman, "Effects of Finite Rates of a Homogeneous Reaction on the Dissolution of Copper in Chloride Solutions," submitted to the *Journal of the Electrochemical Society.*

LAWRENCE BERKELEY LABORATORY
TECHNICAL INFORMATION DEPARTMENT
UNIVERSITY OF CALIFORNIA
BERKELEY, CALIFORNIA 94720